Drug Design, Development and Therapy

Dovepress
open access to scientific and medical research

Open Access Full Text Article

ORIGINAL RESEARCH

Exploration of the Active Component and Mechanisms of Shengyu Decoction Against Myelosuppression Using Network Pharmacology and in vitro Experimental Validation

Bingjie Ma[1], Pengyi Hou[2], Ran Liu[3], Aijun Cang[1], Limei Zhao[4]

[1]Department of Pharmacy, People's Hospital of Liaoning Province, Shenyang, 110010, People's Republic of China; [2]SCIEX Analytical Instrument Trading Co, Shanghai, 200000, People's Republic of China; [3]School of Food and Drug, Shenzhen Polytechnic, Shenzhen, 518000, People's Republic of China; [4]Department of Pharmacy, Shengjing Hospital of China Medical University, Shenyang, 110010, People's Republic of China

Correspondence: Limei Zhao, Department of Pharmacy, Shengjing Hospital of China Medical University, Shenyang, 110010, People's Republic of China, Email lmzhao19@163.com

Background: Chemotherapy-induced myelosuppression (CIM) is a common adverse reaction with a high incidence rate that seriously affects human health. Shengyu Decoction (SYD) is often used to treat CIM. However, its pharmacodynamic basis and therapeutic mechanisms remain unclear.

Purpose: This study aimed to clarify the active components and mechanisms of SYD in CIM.

Methods: LC-QTOF/MS was used to identify the absorbable components of SYD. A series of network pharmacology methods have been applied to explore hub targets and potential mechanisms. Molecular docking was used to identify the binding ability of potential active ingredients and hub targets. Finally, in vitro experiments were performed to validate these findings.

Results: In this study, 33 absorbable prototype components were identified using LC-QTOF/MS. A total of 62 possible targets of SYD in myelosuppression were identified. KEGG pathway enrichment analyses showed that some signaling pathways such as PI3K-Akt and HIF-1 may be the mechanisms by which it functions. Among them, we verified the PI3K-Akt pathway. 6 Hub proteins were screened by Protein–protein interaction (PPI) network analysis. Molecular docking results showed that four absorbable components in SYD showed good binding with six Hub targets. The effectiveness of the four predicted compounds and the mechanism were verified in vitro. It has also been shown that the active component could promote the proliferation of bone marrow stromal cells (BMSCs) and block apoptosis of BMSCs, which may be related to the PI3K-Akt pathway. This result is consistent with the network pharmacology approach and molecular docking predictions.

Conclusion: Our results provided not only the candidate active component of SYD, but also a new insights into mechanism of SYD in the treatment of CIM.

Keywords: Shengyu decoction, SYD, myelosuppression, network pharmacology, molecular docking, active components, mechanism

Introduction

Cancer is a broad group of diseases that involve unregulated cell growth and is internationally acknowledged as one of the main causes of human death and heavily imperiling human life.[1,2] Chemotherapeutic drugs are crucial tools in malignancy treatment and are frequently accompanied by serious side effects.[3,4] Myelosuppression is one of the serious side effects, which may even cause serious mortality problems, making alleviating Chemotherapy-induced myelosuppression (CIM) an important issue in clinical cancer treatments.[5] Currently, the treatment of CIM is mainly symptomatic, including biological agents (colony-stimulating factor, et al) and blood products. However, these drugs may lead to vascular events and lung injury, and even promote cancer development and metastasis.[6] Therefore, the development of a safe and effective drug to treat CIM is imperative.

Received: 11 January 2024
Accepted: 11 June 2024
Published: 20 June 2024

Graphical Abstract

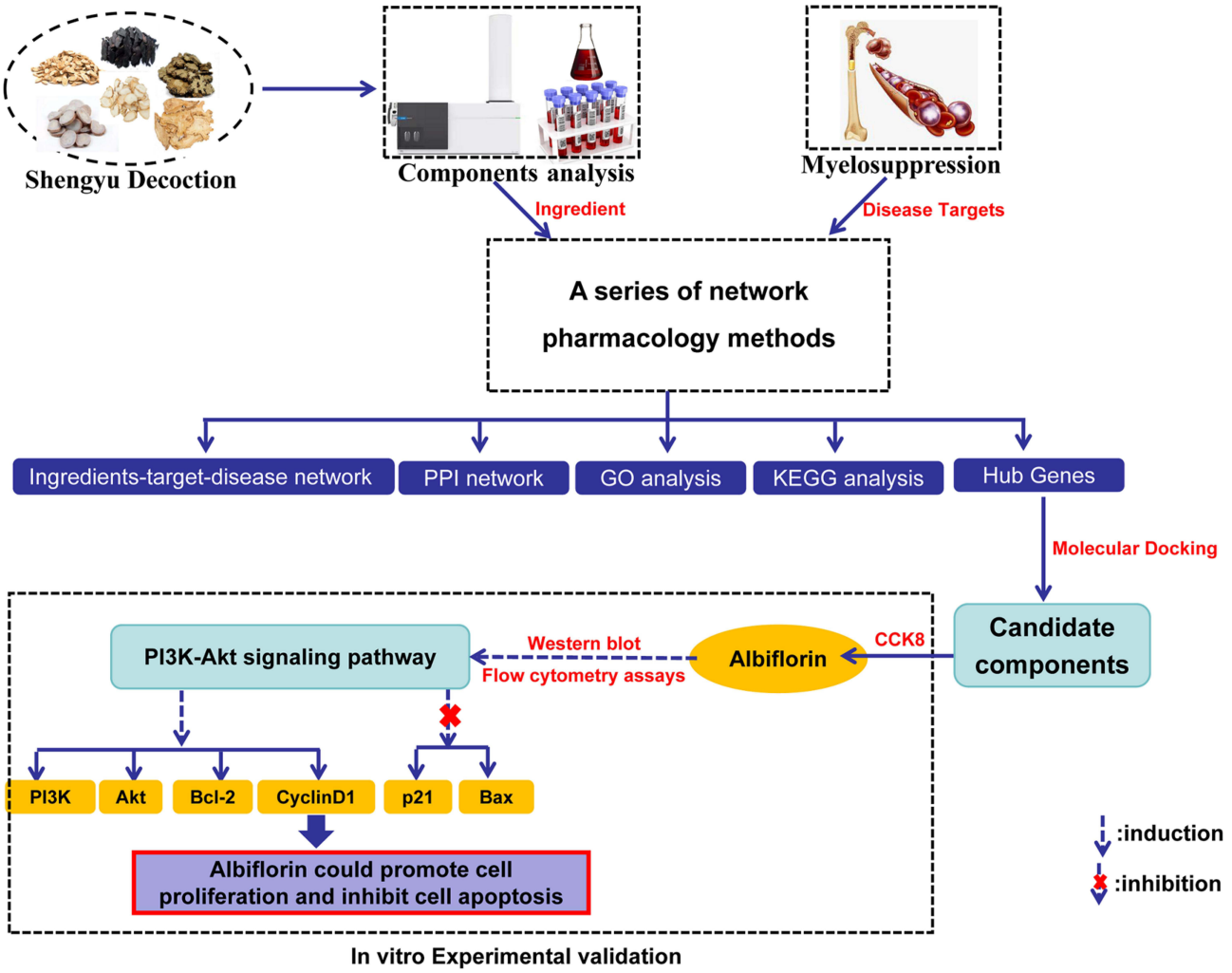

The long-term clinical use of Traditional Chinese medicine (TCM) has led to the accumulation of valuable experience in the treatment of CIM.[7–9] Shengyu Decoction (SYD) is a classical prescription in ancient China, which was first mentioned in Mai Yin Zheng Zhi, a famous medical monograph of the Yuan Dynasty. SYD is believed to treat myelosuppression by replenishing qi and the blood. SYD is composed of six herbs: Radix Rehmanniae Praeparata (shudihuang, SDH), Ginseng (renshen, RS), Radix Paeoniae Alba (baishao, BS), Rhizoma Chuanxiong (Chuanxiong, CX), Radix Angelicae Sinensis (danggui, DG), and Radix Astragali (huangqi, HQ). Studies have revealed that iridoid and phenylpropanoid glycosides are characteristic components of SDH; BS is abundant in monoterpenes; DG and CX are rich in organic acids and essential oils; RS is distinguished by the presence of ginsenosides; And HQ is distinguished by the presence of flavonoids. These extracts and compounds have a broad range of pharmacological activities, such as hemopoietic, immunoregulatory, anti-inflammatory, antibacterial, antiviral, antioxidant, and antitumor activities.[10–13] However, the primary effective substances of SYD against CIM and their regulatory mechanisms remain to be explored.

The multiple constituents of SYD are the advantages of its efficacy, but they also seriously hinder the in-depth understanding of its active substances and the underlying mechanisms for treating CIM. Network pharmacology provides an available tool for elucidating the network synergy of multi-component, multi-pathway, and multi-target between TCM and specific human diseases, which was widely used to elucidate the pharmacological mechanisms of TCM.[14,15] The

molecular docking technology plays an important role in the prediction of docking modes and binding affinities between drug ligands and macromolecule receptors, and it is benefit for predicting the active ingredients of TCM.[16] Therefore, network pharmacology and molecular docking are frequently used complementarily in pharmacological studies of TCM, and their predicted results are then verified experimentally.[17–19] In network pharmacology research, the construction of drug-disease networks usually based on relevant databases. However, the actual composition of TCM is not equal to the sum of the total herbal ingredients in the components database, and only absorbable ingredients can be considered effective ingredients.[20] At present, LC-QTOF/MS is widely applied to the multi-component determination of complex samples, including the detection of TCM compounds and other fields.[21,22] Therefore, the combination of network pharmacology and LC-QTOF/MS can overcome these drawbacks and improve the credibility of the prediction results.

This study aimed to clarify the active constituents and underlying mechanisms of SYD in the treatment of CIM using network pharmacology and molecular docking, followed by experimental validation. Therefore, an LC-QTOF/MS method was established to determine the absorbable components of SYD for use in network pharmacology research. Next, a "compound-target-pathway" network was constructed by network pharmacology to find the key targets and related signaling pathways for treating CIM, and molecular docking was used to screen effective components. Subsequently, the effectiveness of the screened compounds was evaluated. Finally, we validated that the active component of SYD exerts proliferative and anti-apoptotic effects by activating the PI3K-AKT signaling pathway. This study identified the effective ingredients of SYD and the mechanism of action of the components against CIM in vitro, and provided a pharmacological basis for its treatment.

Materials and Methods

LC-QTOF/MS Analysis of SYD Solution and Medicated Rat Serum

Preparation of SYD extract: First, SYD (160 g) was pulverized into fine powders and soaked in 10 times the amount of water for 30 minutes and then boiled for 1 hour. Second, filtered the extraction solution with gauze, then add 8 times and 5 times the amount of water to the filter residue and boil for 1 hour, separately. Third, filtered and combined the extraction solution. Finally, concentrated the extraction solution under reduced pressure to 80mL(2.0 g/mL).

Preparation of SYD-medicated rat serum. Male Wistar rats weighing 220 ± 20 g were obtained from Shenyang Pharmaceutical University Experimental Animal Center. All animal experiments (executed based on the Guidelines for Animal Experimentation of China Medical University) were approved by the Institutional Animal Care and Use Committee of the CMU. Blood samples were collected from the ophthalmic venous plexuses. In our experiments, the rats were randomly divided into 2 groups (n= 6 per group): SYD-containing group and blank group. In the SYD group, rats were gavaged SYD extract (11 g/kg/d). Meanwhile, the same volume of distilled water was gavaged to blank group. All rats were gavaged only once. Rat blood samples were collected 0.5, 1.5, and 3 h after dosing. All serum samples were stored at −80°C until analysis.

Chromatographic conditions: LC-QTOF/MS analysis was performed using an Agilent 1260 HPLC System (Agilent, USA) equipped with a Triple TOF™ 5600+ mass spectrometer (AB SCIEX, USA). HPLC separation was performed on a ZORBAX Eclipse Plus C18 column (150 mm × 4.6 mm, 3.5 μm). A gradient elution program was employed, using 0.1% formic acid in both water (A) and acetonitrile (B) at a flow rate of 0.5 mL/min at 35°C. The injection volume was 4 μL. The gradient program was shown as follows: 5% B at 0–2 min, 5% −15% B at 2–6 min, 15%-25% B at 6–9 min, 25%-30% B at 9–14 min, 30%-33% B at 14–18 min, 33%-40% B at 18–20 min, 40%-95% B at 20–25 min, maintained 95% B at 25-30min, and then maintained 5% B at 30.1-40min.

QTOF/MS conditions: A quadrupole time-of-flight tandem mass spectrometer (QTOF/MS, QTRAP^{TM} 5600+, AB Sciex, USA) was connected to the LC system via an electrospray ionization (ESI) interface. The ionization mode of ESI source adopted positive and negative ionization mode. The optimized conditions were as follows: ion source voltage, 5500V in positive mode and −4500V in negative mode; Declustering potential, 100V in positive mode and −80V in negative mode; collision energy, 30V in positive mode and −30V in negative mode; ion source temperature, 450 °C; The ion source gas1(N_2) and gas2 (N_2) flows were set at 50 psi; curtain gas 30psi.

The operation flow was as follows: Appropriate amount of SYD extract was diluted with methanol to 0.1 g/mL, then filtrated through 0.22 μm microporous membrane for LC-QTOF/MS analysis. To analyze SYD-medicated rat serum, 1 mL of rat serum was added to 3 mL of methanol and vortexed for 3 min to precipitate protein. The sample was centrifuged at 12,000 rpm for 5 min and the supernatant was dried under nitrogen gas at 30 °C. The residue was reconstituted in 100 μL methanol, vortexed for 3 min, and centrifuged at 12,000 rpm for 5 min. The supernatant (4 μL) was injected into the LC-QTOF/MS system and the control blank serum sample was subjected to the same process.

Screening and Target Prediction of SYD Absorbable Ingredients

A total of 33 absorbed compounds of SYD in rat serum were identified using LC-QTOF/MS. Network pharmacology studies have focused on 33 absorbed components. Putative targets of the absorbed compounds in SYD were obtained from the TCMSP and Swiss Target Prediction (taking the top five targets with the score value) databases.

Collection of Gene Targets for Myelosuppression

Myelosuppression-related targets were obtained by searching the keywords "myelosuppression" and "bone marrow suppression" in the OMIM (https://omim.org/) and GeneCards (https://www.genecards.org/) databases, respectively. Gene names were calibrated using UniProt database (https://www.uniprot.org/). Finally, we merged the data and removed duplicate content.

Collection of Potential Targets for SYD Treatment of Myelosuppression

Venny 2.1 (https://bioinfogp.cnb.csic.es/tools/venny/index.html) was used to plot a Venn diagram of the interaction between the targets of SYD and the disease targets of myelosuppression. The common targets of both were used as potential targets for the SYD treatment of myelosuppression.

Construction of Component-Target Network

For visualization, the potential active compounds of SYD and their potential effector targets were entered into Cytoscape 3.8.2 software to draw the "SYD-compound-target" network analysis diagram.

Construction of Protein-Protein Interaction (PPI) Network and Screening of Core Targets

The common gene targets of SYD and myelosuppression were uploaded to the STRING database (https://string-db.org/), in which the biological species were selected as "homosapiens" and all other parameters were default values. PPI network results were imported into Cytoscape 3.8.2. MCODE and Cytohubba plug-ins were used to identify core targets.

Enrichment Analysis

GO enrichment analysis, including biological process (BP), cellular component (CC), and molecular function (MF), and KEGG pathway enrichment analysis were performed on key targets using the DAVID Database (https://david.ncifcrf.gov/). The top 10 items in the GO analysis and the TOP 20 items in the KEGG analysis were selected and visualized. According to Fisher's test, statistical significance was set at $p<0.05$.

Molecular Docking

SMILES files of small-molecule compounds were downloaded from the PubChem database and converted to mol2 format using Discovery Studio 2020 software. The 3D structures of the core targets were obtained from the Protein Data Bank database (PDB) (http://www.rcsb.org/).

First, the iGEMDOCK molecular docking software was used to quickly screen compounds with a good binding capacity with six core proteins. Select "standard docking" for docking mode, and all other parameters are set to default values. A total binding energy of less than −90 kJ/mol was considered as the criterion for stable binding, and the components that had good binding with all six core proteins were initially identified as the key components.

Then, the selected key components with core proteins were accurately docked and visualized using AutodockTool 1.5.6 and PyMol software. OpenBabel 3.1.1 were used to convert the SDF format of key components to mol2 format, and the mol2 format of the ligands was input into AutoDockTools 1.5.6, to add polar hydrogen atoms and Gasteiger charges and output them in pdbqt

format. Proteins were de-liganded, dehydrated, and hydrogenated in AutoDockTools 1.5.6, and output as files in the pdbqt format. The pdbqt files of the ligands and receptors were imported into the AutoDockTools 1.5.6. When the docking box was constructed, the receptor proteins were centered, the docking boxes completely covered the receptor proteins, and the ligands were located outside the docking box. Molecular docking was performed using AutoDockTools 1.5.6, and a total binding energy less than −0 kJ/mol was used as the criterion for stable binding. The components that had good binding with all six core proteins were considered as effective components. The results of molecular docking were visualized using PyMOL software.

Reagents and Cell Culture

Calycosin-glucoside and ferulic acid were purchased from the National Institutes for Food and Drug Control (Beijing, China), while 5-FU, LY294002, albiflorin, and paeoniflorin were purchased from MCE (Shanghai, China).

The Mouse bone marrow stromal cell line (OP9) (Shanghai Institute of Biological Sciences, Chinese Academy of Science, Shanghai, China) was maintained in DMEM (BI, USA) with 10% FBS (BI, USA) in a 5% CO_2 humidified 37°C incubator. Fresh medium was added to the cells every 2–3 days.

Validation of Active Ingredients

Cells were divided into control, model, and treatment groups. The treatment groups were further divided into four groups: ferulic acid, calycosin-7-glucoside, albiflorin, and paeoniflorin groups. The control group was cultured as a routine for 24 h, and the model group was treated with 25 μg/mL 5FU for 24 h. Treatment groups were cultured with 25 μg/mL 5FU and different compounds at different concentrations for 24 h: ferulic acid (10, 20, 40, 60 μmol/mL), calycosin-7-glucoside (10, 20, 40, 60 μmol/mL), albiflorin (10, 40, 80, 160 μmol/mL), and paeoniflorin (5, 10, 20, and 40 μmol/mL). Cell proliferation assays were performed using Cell Counting Kit-8 (CCK8).

Validation of the Mechanism of Action Based on the PI3K-Akt Pathway

Cell grouping and treatments. Cells were divided into five groups: control group, 5FU group, albiflorin group, albiflorin +LY294002 group, and LY294002 group. Control group was cultured as routine; all cells except the control group were cultured with 5FU (25 μg/mL) and different drugs for 24 h: albiflorin group was cultured with albiflorin (40 μmol/mL); albiflorin +LY294002 group was cultured with albiflorin (40 μmol/mL) and LY294002 (50 μM); LY294002 group was cultured with LY294002 (50 μM).

Flow cytometry assays. Cell apoptosis and cell cycle analyses were performed using flow cytometry. Cell pellets from different groups were collected separately, digested with 0.25% trypsin for 2 min, and washed with PBS buffer at 37°C. Apoptosis of OP9 cells was evaluated using an Annexin V-FITC/PI Apoptosis Kit (Annoron, Beijing, China). OP9 cells were resuspended in 200 μL binding buffer and double-stained with Annexin V-FITC and PI (Thermo Fisher, USA) for 15 min in the dark. For cell cycle analysis, cells were fixed with 70% ice-cold ethanol overnight at −20°C, then added 500 μL cycle reagent (Millipore, USA) and incubated for 30 min at room temperature. Subsequently, OP9 cells were analyzed using a flow cytometer (EC201827C1; Luminex, USA) and FlowJo software v.7.6 (FlowJo LLC, USA).

Western blotting. Total protein was extracted from OP9 cells using RIPA buffer (Beyotime Biotech, Shanghai, China) supplemented with 0.05% phosphatase inhibitors (Beyotime Biotech). The Membranes were blocked by TBST with 5% non-fat dry milk and incubated overnight at 4°C with anti-PI3K, p-PI3K, Akt, p-Akt, p21, cyclin D1, Bax, Bcl-2, GAPDH (Cell Signaling Technology, Beverly, Massachusetts, USA). Blots were visualized using ECL reagents (Millipore, Bedford, MA, USA) and the bands were scanned and quantified using ImageJ software. The relative expression levels of target proteins were normalized to those of GAPDH and β-actin.

Statistical Analysis

Statistical analyses were performed using the SPSS software (version 20.0; SPSS, Chicago, USA). For continuous data, data normality was tested by Q-Q plots and the homogeneity of variance was performed by Levene's test. Normally distributed variables were presented as mean ± standard deviation (Mean ± SD), one-way analysis of variance (ANOVA) and Tukey's post hoc test were used if variance was equal, and the Welch ANOVA and Games-Howell hoc test were used if variance was

not equal to compare the groups. Non-normally distributed data were presented as median (M) and inter-quartile range (IQR) and were analyzed by Kruskal–Wallis test and Bonferroni's post hoc test. $p < 0.05$ was considered statistically significant.

Results

LC-QTOF/MS Analysis of SYD Solution and Medicated Rat Serum

Ingredients in SYD solution: First, a reference database including the chemical name, structural formula, relative molecular mass, and characteristic fragments was constructed for SYD. Information was collected from the PubMed, SciFinder databases, and other researchers. In addition, unique neutral-loss molecules and/or the characteristic fragment ions of each type of component were obtained. Second, two specific data processing methods of PeakView® V. 2.2 Workstation, neutral loss filtration (NLF) and sub ion filtration (PIF), were used to identify the components in SYD, which two further helped to find and predict the compounds with specific neutral loss molecules and characteristic fragment ions effectively. Classified the possible components in SYD based on the constructed chemical information database. After obtained the unique neutral loss molecules and/or characteristic fragment ions to each type of component, NLF and PIF screening were performed. Finally, the structure of the compound was predicted based on the obtained effective information. In total, 148 compounds were identified. The total ion flow chromatography (TIC) under positive and negative ion modes and the identified 148 compounds are shown in Supplementary Figure 1 and Supplementary Table 1, respectively. The proposed fragmentation patterns of the typical compounds are shown in Supplementary Figure 2.

Ingredients in SYD-medicated rat serum: The components detected in the serum samples were compared with those in SYD solution. If the chromatographic and mass spectrometric characteristics of compounds in the serum are consistent with those of compounds in the SYD solution, they are considered potential medicinal ingredients. Finally, 33 components were absorbed as the prototypes. Detailed information on the identified 33 compounds is shown in Supplementary Table 2 and the TIC are shown in Supplementary Figure 3.

Collection of component targets for SYD and disease targets for myelosuppression.

A total of 33 absorbable compounds were identified using LC-QTOF/MS and retrieved from the TCSMP and Swiss Target Prediction databases. Of these, 5 compounds were not present in the above databases. After removing duplicate contents, 113 compound-related targets were identified. A total of 2946 myelosuppression targets were identified by searching and screening the GeneCards and OMIM databases. A total of 62 intersection targets for components and diseases were drawn using Venny 2.1.0. The intersecting targets were considered as potential targets for SYD treatment of CIM in the next step of the analysis (Figure 1).

Construction of the SYD-Active Ingredient-Target Network

The 62 intersection targets and the corresponding 28 compounds were imported into Cytoscape 3.8.2 software to construct an active ingredient-target network for image visualization and analysis. The network contained 113 nodes

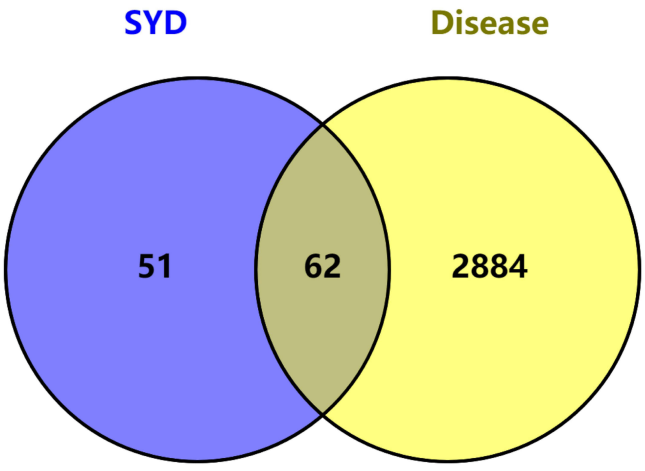

Figure 1 The intersection of Sheng-Yu decoction (SYD) and myelosuppression targets.

and 248 edges (Figure 2). Among them, one compound can interact with multiple targets, and different compounds can act on the same target simultaneously. This reflects the multi-component and multi-target effects of SYD.

GO and KEGG Enrichment Analysis

Through GO enrichment analysis, the potential BP, CC, and MF of the 62 target genes were identified. These Results suggest that SYD may be involved in the biological processes of negative regulation of apoptosis and the positive regulation of cell proliferation in the treatment of myelosuppression. The potential signaling pathways of the 62 target genes were identified using KEGG enrichment analysis. A total of 111 significantly enriched signaling pathways were identified, and the top 20 significantly enriched signaling pathways are shown in Figure 3. The results showed that the main signaling pathways related to myelosuppression were enriched in the PI3K-Akt, HIF-1, VEGF, and estrogen pathways.

Construction of the PPI Network and Cluster Analysis

As shown in Figure 4A, the PPI network consisted of 58 nodes (4 targets were not involved) and 374 edges. The "edges" represent the interrelationship between the targets and indicate the degree of association. Therefore, the larger the node, the higher is the degree of association between the corresponding target and other targets. Cluster analysis was conducted using the MCODE plug-in of Cytoscape 3.8.2, to obtain subnetworks with the highest scores, in which all 18 genes were considered to play an important role in the PPI network (Figure 4B). The Cytohubba plug-in was used to identify hub genes. As shown in Figure 5, the darker the color of the gene in the figure, the higher is the degree of association between other genes. Genes with high scores in all the six algorithms were identified as hub genes. Finally, TNF, IL-6, VEGFA, SRC, HRAS, and STAT3 were identified as hub genes and used as potential core targets for the next analysis.

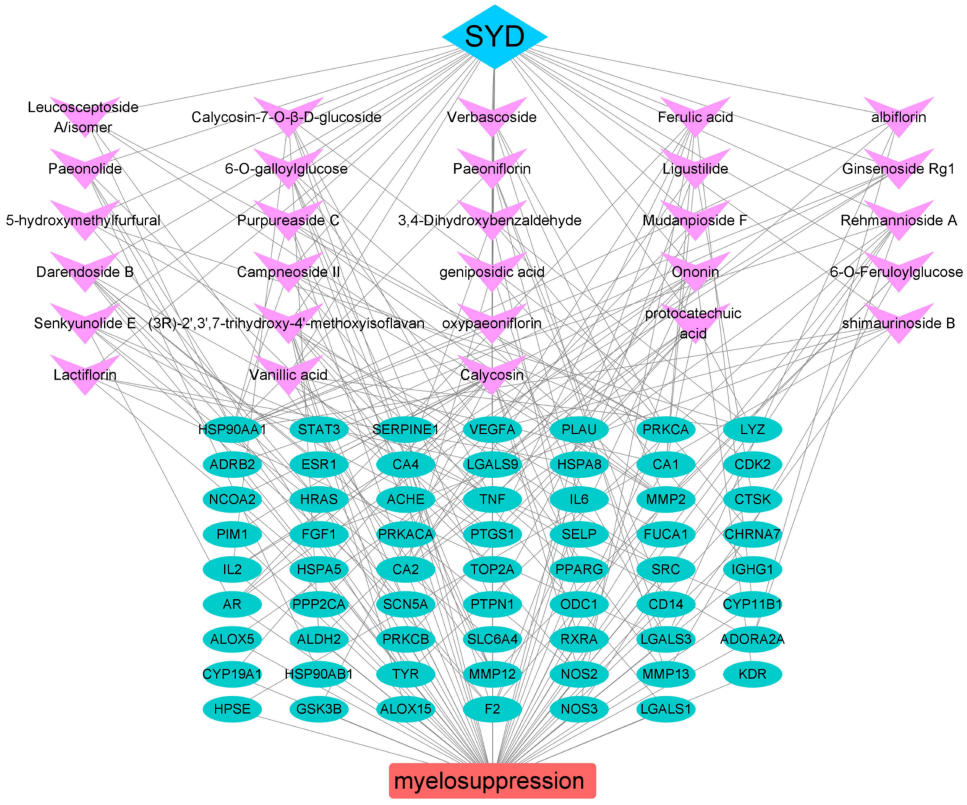

Figure 2 The Chinese medicine-compound-target-disease network.

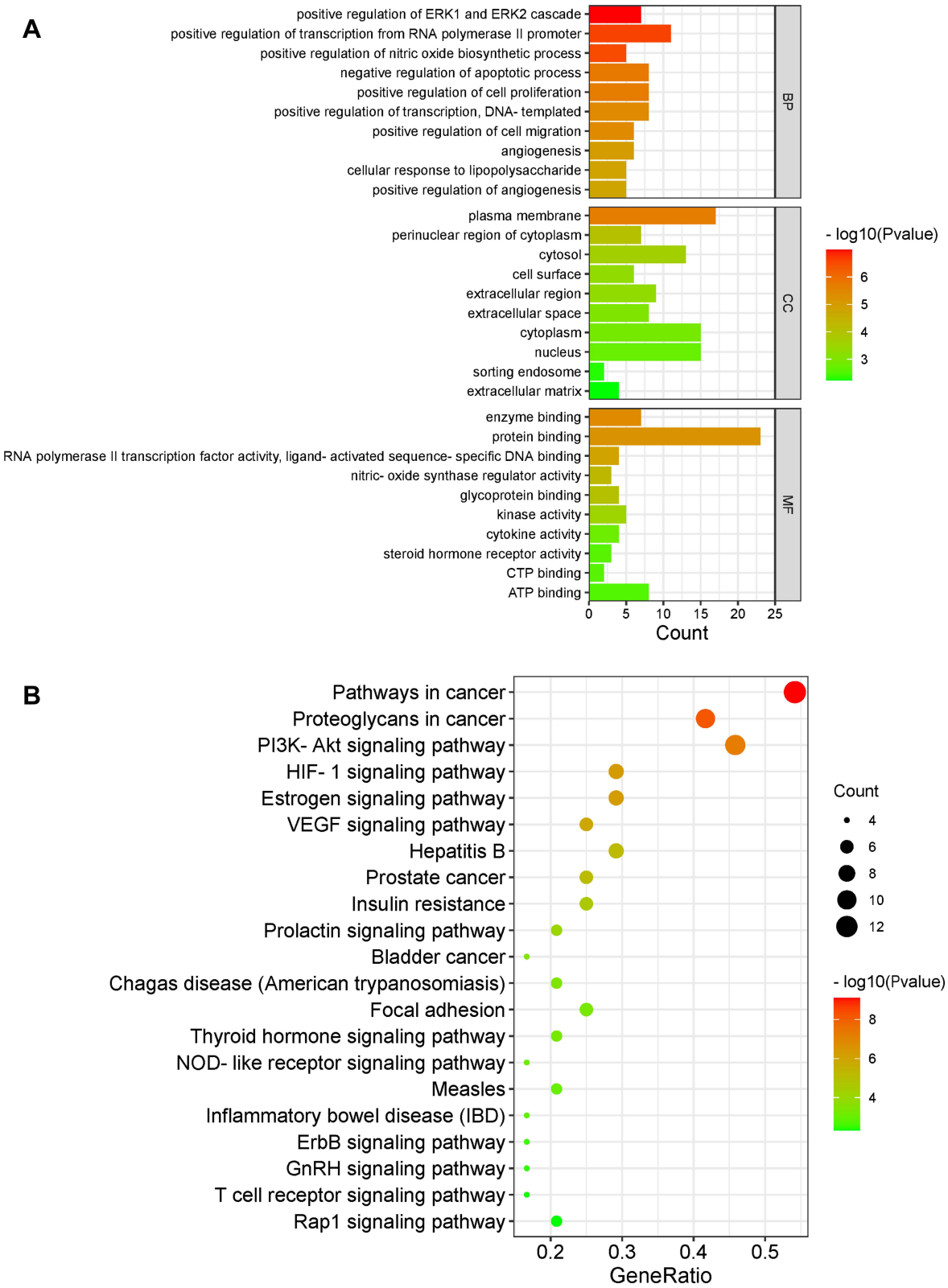

Figure 3 The top 10 pathways for GO analysis (**A**) and the top 20 pathways for KEGG analysis (**B**) of the targets of SYD.

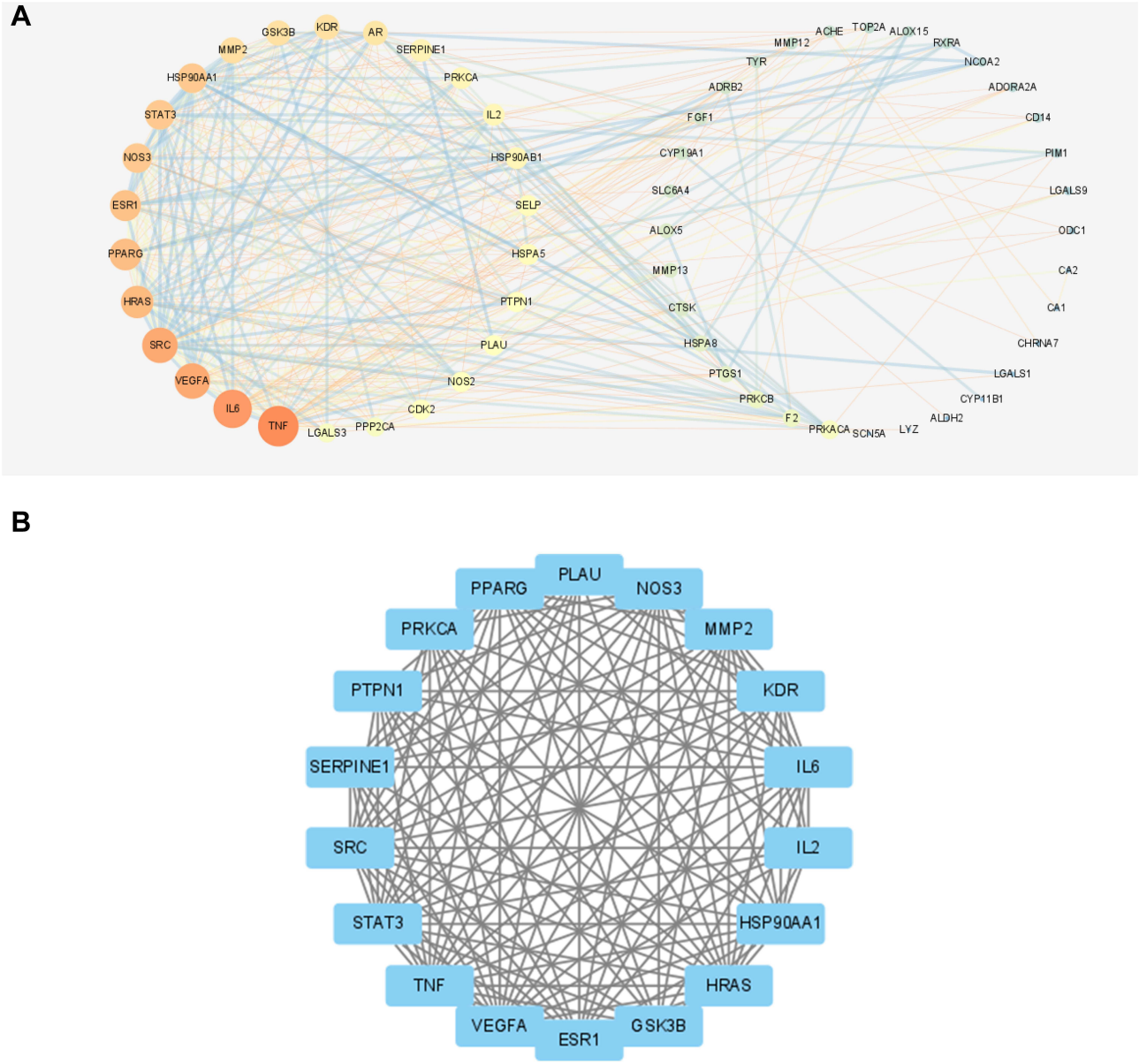

Figure 4 The PPI network of interaction targets (**A**) and subnetworks with the highest score (**B**).

Molecular Docking Results

The 28 compounds in the SYD-active ingredient-target network were molecularly docked with six core targets using iGEMDock v2.1. The lower the binding energy, the more stable is the conformation of the ingredient that binding to the target. The results indicated that 10 compounds, including Campneoside II, darendoside B, leucosceptoside A, purpureaside C, verbascoside, ferulic acid, calycosin-7-glucoside, albiflorin, paeoniflorin, and oxypaeoniflorin, had relatively high binding potential to the core targets.

Subsequently, AutoDockTool 1.5.6 software was used to further screen the active ingredients of the 10 compounds mentioned above, and the results are shown in Supplementary Table 3. The results showed that ferulic acid, calycosin-7-glucoside, albiflorin, paeoniflorin, and oxypaeoniflorin had lower affinities, demonstrating that they have a higher possibility of binding to core targets, suggesting that they may be the active ingredients of SYD in the treatment of myelosuppression. Representative molecular docking mode diagrams are presented in Supplementary Figure 4.

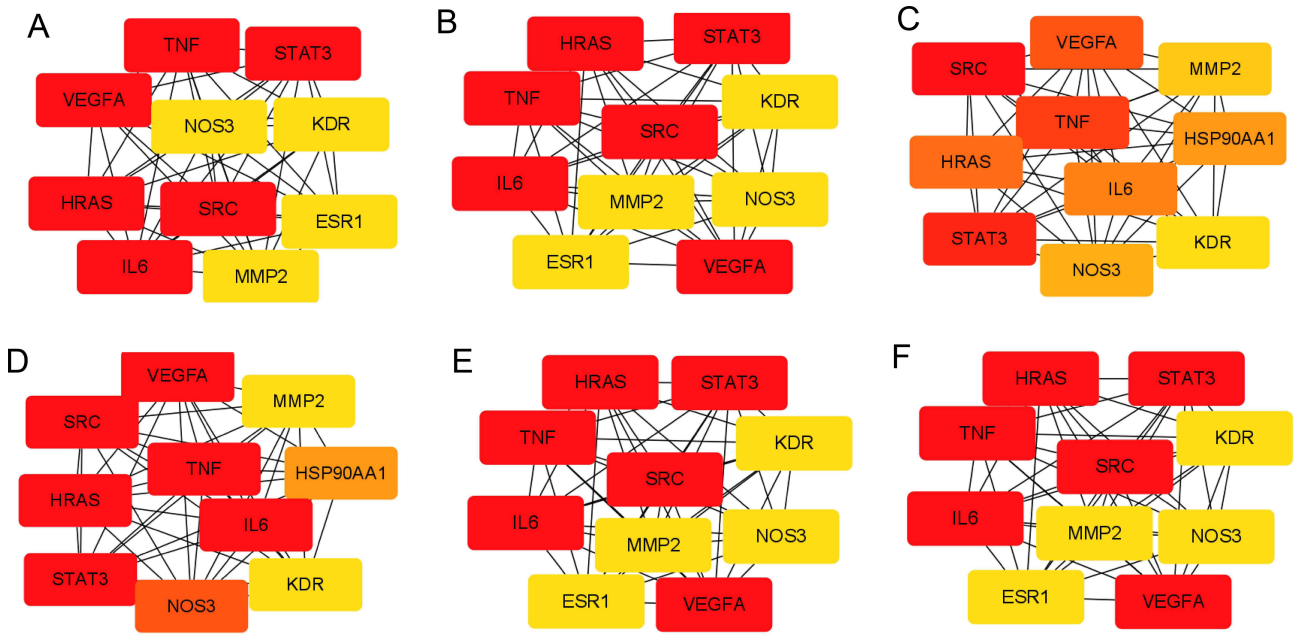

Figure 5 The hub genes screened by Cytohubba plug-in in six algorithms. (**A**) The algorithm of Closeness; (**B**) The algorithm of Degree; (**C**) The algorithm of EPC; (**D**) The algorithm of MCC; (**E**) The algorithm of MNC; (**F**) The algorithm of radiality.

In vitro Experiments Results

Combined with the results of molecular docking and related literature, calycosin-glucoside, albiflorin, ferulic acid, and paeoniflorin were preliminarily selected as the active ingredients. The CCK8 method was used to detect the effects of the four predicted components on the cell proliferation activity of OP9 cells. Based on the CCK8 results, albiflorin with the strongest activity was selected for the next study. Furthermore, Western blot and flow cytometry were used to verify the regulatory effects of albiflorin on the PI3K-Akt signaling pathway in OP9 cells.

Active ingredients alleviated the inhibitory effect of 5-FU on bone marrow stromal cells (BMSCs) proliferation.

As shown in Figure 6, compared to the control group, the proliferation of OP9 cells was significantly decreased after treated with 5-FU. Compared to the 5-FU group, after the co-cultured compounds reached a certain concentration, all four compounds obviously increased the proliferation activity of OP9 cells ($p < 0.05$). The activity of albiflorin (40 μM) was the highest.

Albiflorin promote the growth of OP9 cells by stimulating PI3K-Akt signaling pathway.

Effects of albiflorin on apoptosis and cell cycle in OP9 Cells. As shown in Figure 7, compared with the 5-FU group, after co-culture with 5-FU and albiflorin (5-FU+albiflorin group), the proportion of cells in the G0/G1 phase and the apoptosis ratio significantly decreased ($p < 0.05$) and remarkably increased the proportions in the S, G2/M phase, and PI ($p < 0.05$). In addition, the expression of Bcl-2 and Cyclin D1 increased significantly, whereas that of BAX and p21 decreased significantly ($p < 0.05$). Albiflorin may rescue OP9 cell growth inhibition after 5-FU treatment by inhibiting apoptosis and promoting proliferation.

The 5-FU group and 5-FU+albiflorin group were compared with the 5-FU+LY294002 group and 5-FU+albiflorin +LY294002 group, respectively. It was found that after co-culturing with LY294002, an inhibitor of the PI3K-Akt signaling pathway, the apoptosis ratio increased significantly ($p < 0.05$), and the proportions of the S, G2/M phase, and PI decreased remarkably ($p < 0.05$). Moreover, the expression of Bcl-2 and Cyclin D1 decreased significantly, whereas that of BAX and p21 increased significantly ($p < 0.05$). This indicates that the PI3K-Akt pathway may be inhibited by 5-FU, and albiflorin could reverse the inhibitory effect of 5-FU.

The effects of albiflorin on the expression of proteins related to the PI3K-Akt signaling pathway. As shown in Figure 8, compared with the control group, the expression of PI3K, p-PI3K, Akt, and p-Akt decreased significantly in 5-FU group; compared with the 5-FU group, the expression of p-PI3K, Akt, and p-Akt further remarkably increased in

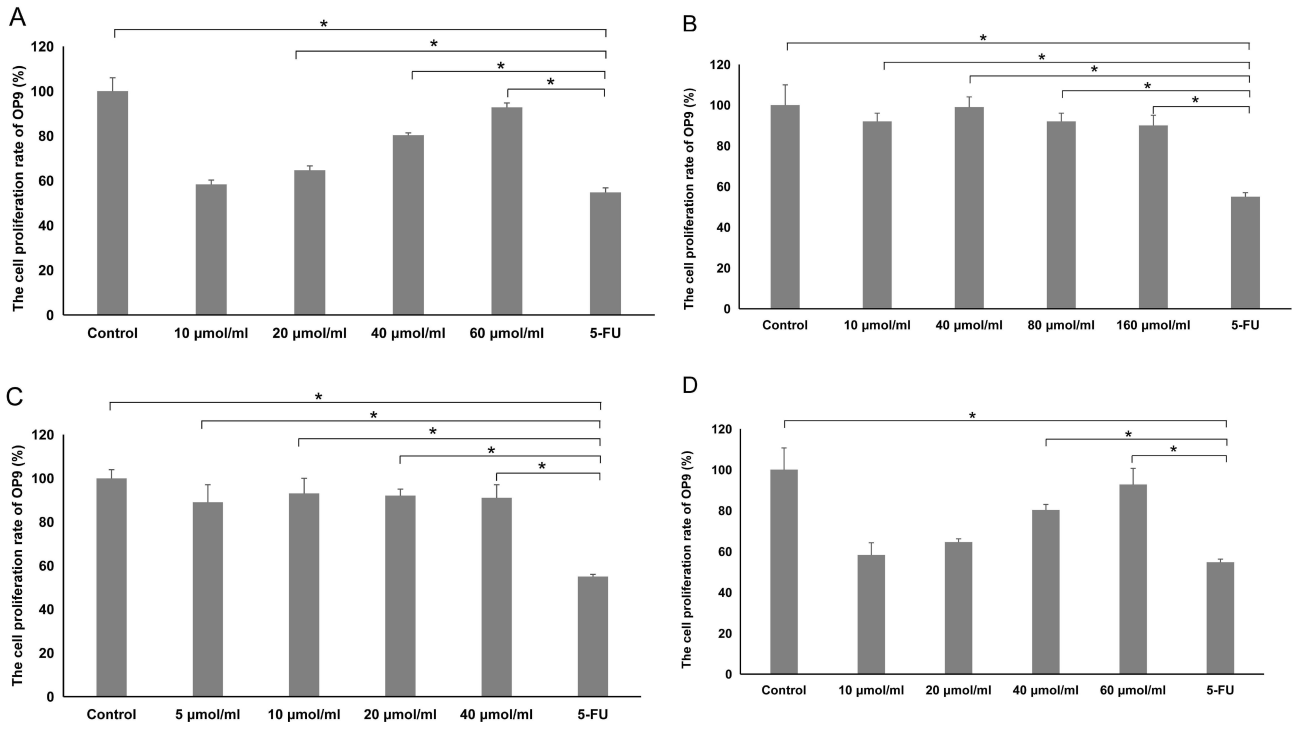

Figure 6 Proliferation activity of OP9 cells after treated with four active ingredient at different concentration. (**A**) Effects of calycosin-glucoside on the proliferation activity of OP9 Cells. (one-way ANOVA. Compared with the 5-FU group, the *p*-values of the control, 10μmol/mL, 20μmol/mL, 40μmol/mL and 60μmol/mL groups were 0.000064, 0.939, 0.001, 0.00008 and 0.000375, respectively). (**B**) Effects of albiflorin on the proliferation activity of OP9 Cells. (one-way ANOVA. Compared with the 5-FU group, the *p*-values of the control, 10μmol/mL, 40μmol/mL, 80μmol/mL and 160μmol/mL groups were 0.000001, 0.00005, 0.000001, 0.000076 and 0.000225, respectively). (**C**) Effects of paeoniflorin on the proliferation activity of OP9 Cells. (Welch ANOVA. Compared with the 5-FU group, the *p*-values of the control, 5μmol/mL, 10μmol/mL, 20μmol/mL and 40μmol/mL groups were 0.000028, 0.011, 0.003, 0.000018 and 0.000267, respectively). (**D**) Effects of ferulic acid on the proliferation activity of OP9 Cells. (Welch ANOVA. Compared with the 5-FU group, the *p*-values of the control, 10μmol/mL, 20μmol/mL, 40μmol/mL and 60μmol/mL groups were 0.002, 0.835, 0.058, 0.000005 and 0.001, respectively). (**A**–**D**) All data are shown as mean ± SD, $n = 6$ per group. *$p < 0.05$.

5-FU+albiflorin group; 5-FU group and 5-FU+albiflorin group were compared with 5-FU+LY294002 group and 5-FU +albiflorin+LY294002 group respectively, it was found that after co-culture with LY294002, the expression of PI3K, p-PI3K, Akt, and p-Akt decreased significantly. These results further illustrate that the myelosuppression induced by 5-FU may be related to the PI3K-Akt pathway, and that albiflorin could activate the PI3K-Akt pathway to relieve myelosuppression.

Discussion

Myelosuppression is one of the main adverse effects of chemotherapy.[23] Most patients with cancer experience different degrees of myelosuppression due to chemotherapy and/or radiotherapy. Consequently, an effective treatment for CIM is urgently needed. In recent years, TCM has been widely used as integrative therapy for cancer treatment. Several studies have shown that TCM can prevent CIM.[24–26] However, TCM often contains multiple components, and the effects of each component are often complex, leading to the predicament of unclear pharmacological mechanisms in the development of TCM. SYD, a classic TCM formula with low toxicity and multi-target characteristics, is widely used as a complementary therapy to alleviate CIM. However, studies on the active components and mechanisms of SYD in CIM treatment are lacking. Therefore, this study aimed to clarify the active ingredient and mechanism of SYD in CIM and further validate the presume predicted by network pharmacology and molecular docking using in vitro experiments.

First, we identified 148 compounds in the SYD using LC-QTOF/MS. Although SYD contains many ingredients, only a few ingredients with drug-likeness can be absorbed to produce therapeutic effects. Therefore, after identified the chemical components of the SYD extract, the absorbable components were identified. Finally, we preliminarily identified the 33 components absorbed as a prototype. According to previous reports, many absorbable compounds in SYD could promote hematopoiesis.[27–30] Rehmannia Radix polysaccharides are the main components of SDH. Rehmannia Radix

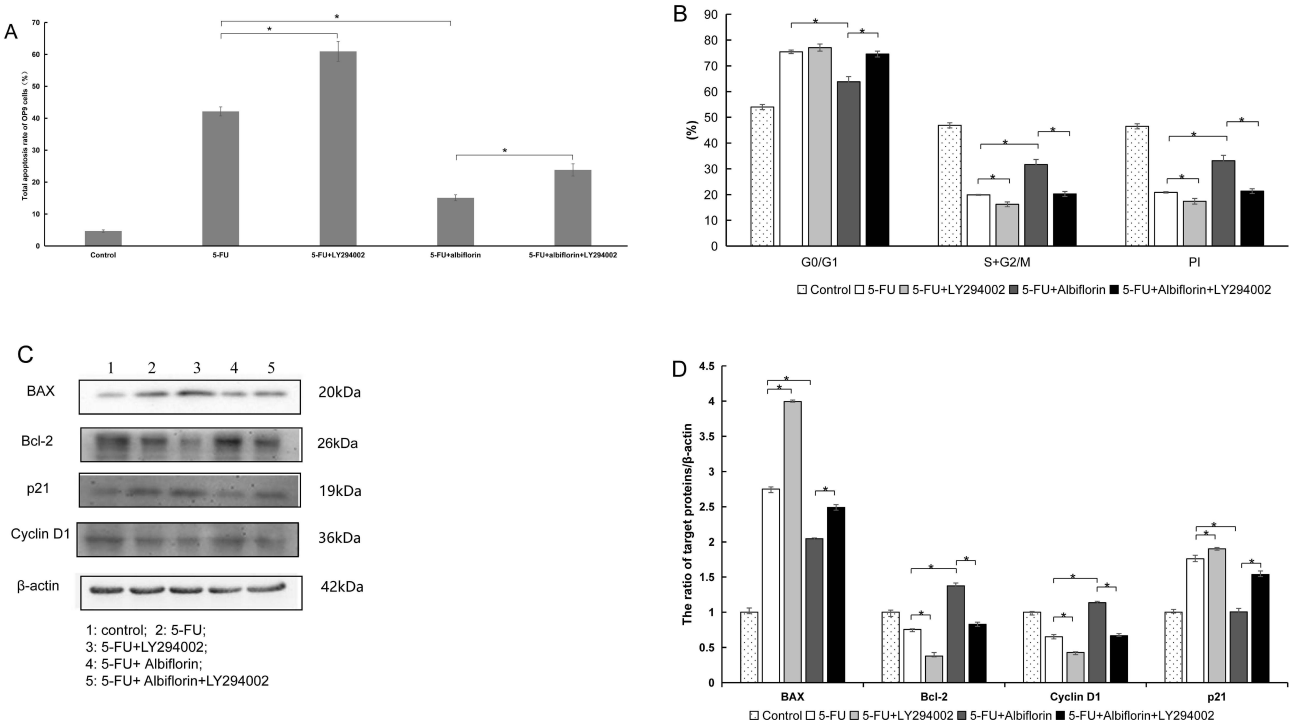

Figure 7 (**A**) Apoptosis of OP9 cells under different treatment conditions. (Welch ANOVA, the *p*-values were 0.000065, 0.000002, and 0.000054, respectively). (**B**) Cell cycle of OP9 cells under different treatment conditions. (G_0/G_1: one-way ANOVA, the *p*-values were 0.603, 0.00008, and 0.000017, respectively. $S+G_2/M$: Welch ANOVA, the *p*-values were 0.041, 0.027, and 0.013, respectively. PI: one-way ANOVA, the *p*-values were 0.034, 0.00002, and 0.00002, respectively.) (**C**)The effect of albiflorin on the protein expression of BAX, Bcl-2, Cyclin D1 and p21 proteins in OP9 cells under different treatment conditions. (**D**) Gray value statistics of BAX, Bcl-2, Cyclin D1, p21. (BAX: Welch ANOVA, the *p*-values were 0.000011, 0.000002, and 0.000022, respectively. Bcl-2: Welch ANOVA, the *p*-values were 0.000479, 0.000504, and 0.01, respectively. CyclinD1: Welch ANOVA, the *p*-values were 0.000084, 0.000007, and 0.000005, respectively. P21: one-way ANOVA, the *p*-values were 0.000014, 0.000007, and 0.00045, respectively.). Control: treated as normal; 5-FU: treated with 5-FU (25 μg/mL); 5-FU+LY294002: treated with 5-FU and LY294002 (50 μM); 5-FU+albiflorin: treated with 5-FU and albiflorin (40 μmol/mL); 5-FU+albiflorin +LY294002: treated with 5-FU, LY294002 and albiflorin. (**A, B** and **D**) All data are shown as mean ± SD, *n* = 6 per group. The order of p-values is 5-FU group and 5-FU+LY294002 group, 5-FU group and 5-FU+albiflorin, and 5-FU+albiflorin group and 5-FU+albiflorin+LY294002 group. **p* < 0.05.

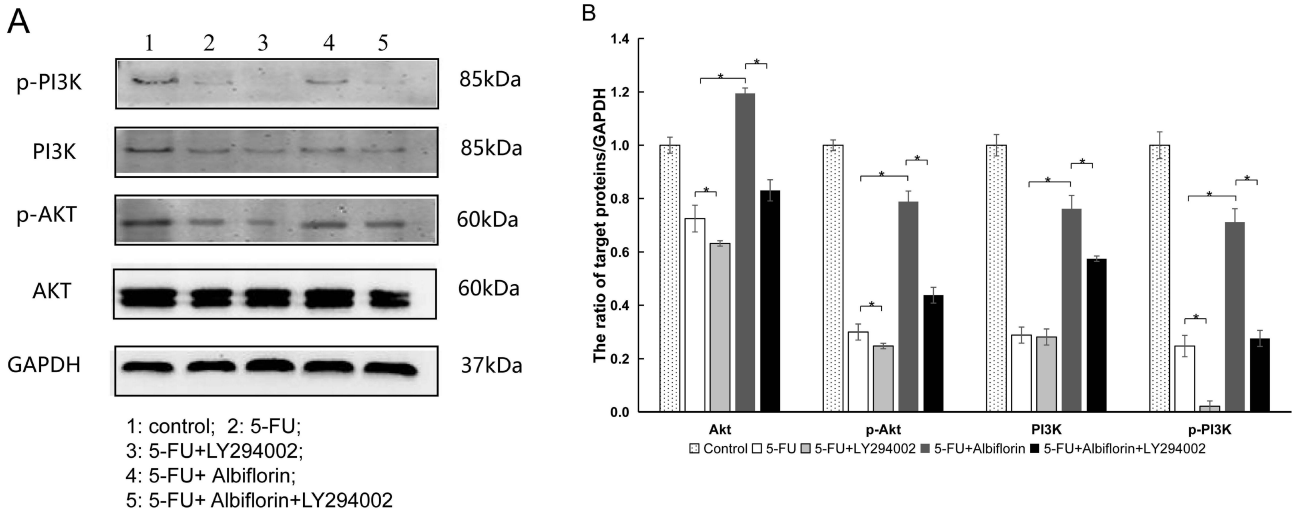

Figure 8 The effect of albiflorin on the protein expression of PI3K-Akt pathway-related proteins in OP9 cells under different treatment conditions: Control: treated as normal; 5-FU: treated with 5-FU (25 μg/mL); 5-FU+LY294002: treated with 5-FU and LY294002 (50 μM); 5-FU+Albiflorin: treated with 5-FU and albiflorin (40 μmol/mL); 5-FU+Albiflorin+LY294002, treated with 5-FU, LY294002 and albiflorin. (**A**) Representative immunoblotting images of p-PI3K, PI3K, Akt, p-Akt, and GAPDH; (**B**) Gray value statistics of p-PI3K, PI3K, Akt, p-Akt. (Akt: Welch ANOVA, the *p*-values were 0.007, 0.000052, and 0.000001, respectively. p-Akt: one-way ANOVA, the *p*-values were 0.011, 0.000428, and 0.000048, respectively. PI3K: one-way ANOVA, the *p*-values were 0.946, 0.0014, and 0.000013, respectively. p-PI3K: Welch ANOVA, the *p*-values were 0.007, 0.021, and 0.024, respectively.). All data are shown as mean ± SD, *n* = 6 per group. The order of p-values is 5-FU group and 5-FU+LY294002 group, 5-FU group and 5-FU +albiflorin, and 5-FU+albiflorin group and 5-FU+albiflorin+LY294002 group. **p* < 0.05.

polysaccharides increase the self-renewal ability of long-term HSCs and maintain Lin-Sca1+c-kit- cell quiescence by upregulating p18 expression. It also decreased the level of reactive oxygen species and the percentage of β-gal+ cells by downregulating the cellular senescence-associated proteins, p53 and p16. Thus, it plays a role in delaying aging and promoting HSC proliferation. Monoterpene glycosides are the main components of BS, which can increase the levels of GM-CSF, G-CSF, and IL-3, as well as reduce the levels of TNF-α in the serum, indicating that they promote hematopoiesis. Organic acids and polysaccharides were the main water-soluble components of DG and CX, respectively. Studies have shown that ferulic acid can increase the levels of G-CSF and EPO, which can enhance the activity of HSCs and accelerate the recovery of blood cells. Angelica sinensis polysaccharides (ASP) can delay senescence in HSCs, which may be partly due to the inhibition of oxidative damage and the downregulation of p16 mRNA expression. In addition, ASP protects BMSCs from chemotherapeutic injury by inhibiting oxidative damage to stromal cells and by improving their hematopoietic microenvironment. Ginsenosides are the main components of ginseng, which can regulate different signaling pathways (ie, Wnt/β-Catenin and SIRT6/NF-κB signaling pathways), suppress oxidative stress, and reduce the expression of p16INK4a, p19Arf, and other aging-related proteins to delay senescence of HSCs. In addition, it can improve the hematopoietic microenvironment and enhance immunity. Flavonoids are the main components of HQ, which can regulate the cytokines IL-2, IL-6, GM-CSF, and TNFα in the serum, exhibiting protective effects against myelosuppression, probably by attenuating oxidative stress, promoting cell proliferation, and inhibiting apoptosis. Overall, the absorbed components of SYD promoted bone marrow cell proliferation and reduced cell apoptosis by regulating different signaling pathways or improving the hematopoietic microenvironment by regulating the expression of LN, FN,VCAM-1, and other proteins on the surface of BMSCs. This study preliminarily clarifies the main chemical material basis of SYD and lays the foundation for an in-depth study of its pharmacodynamic substance basis and quality control methods.

To further investigate the mechanism of SYD intervention in the myelosuppression process, we first considered the identified absorbable components as potential active ingredients of SYD for CIM and screened the molecular mechanisms using network pharmacology. A total of 62 key targets of SYD acting on myelosuppression were identified, and six proteins that were considered the core targets of SYD in treating myelosuppression were screened through PPI network and cluster analysis, including IL-6, TNF, SRC, HRAS, STAT3, and VEGFA. Studies have shown that these targets could affect the hematopoietic function of the bone marrow through different pathways.[31,32] IL-6 is a pleiotropic cytokine secreted by BMSCs, which could promote the proliferation and differentiation of HSCs. IL-6 can act on early HSCs, causing the proliferation of erythroid and myeloid progenitors in the bone marrow and increasing the number of red blood cells, granulocytes, and platelets in the peripheral blood. In addition, IL-6 cooperates with IL-3 to stimulate HSCs to enter the cell proliferation cycle, leading to an increase in early HPCs. VEGFA is produced by various cells in the bone marrow microenvironment, and its expression is regulated by multiple factors such as growth factors, hypoxia, cytokines, and hypoglycemia. During the hematopoietic process, the survival and function of HSCs in the bone marrow is regulated by VEGFA. The results of GO and KEGG analyses showed that SYD was related to biological processes, such as negative regulation of apoptosis and positive regulation of cell proliferation, and the main pathways related to myelosuppression were enriched in the PI3K-Akt, HIF-1, VEGF, and estrogen pathways. The PI3K-Akt signaling pathway is an intracellular signaling pathway that plays an important role in maintaining and improving hematopoiesis. Studies have shown that the PI3K-Akt pathway can affect the apoptosis of BMSCs by regulating the activity of Caspase-3, and the processes of proliferation, apoptosis, and autophagy in the production of erythrocytes by regulating EPO/EPOR.[33] In addition, PI3K-Akt signaling pathway plays an important role in maintaining homeostasis and differentiation of HSCs. The abnormal inactivation of the PI3K-Akt signaling pathway causes HSCs to remain in the G0 phase, lose hematopoietic differentiation ability, and hinder the differentiation of B cells, thereby causing serious damage to the function of HSCs.[34,35]

Molecular docking results showed that ferulic acid, oxypaeoniflorin, paeoniflorin, albiflorin, and calycosin-7-O-glucoside may be the key compounds in the treatment of myelosuppression. These ingredients have been proven to have potential advantages in affecting hematopoiesis through different pathways.[36–39] Paeoniflorin and albiflorin could increase the levels of GM-CSF, C-CSF, and IL-3 in serum or plasma, and reduce the level of TNF-α in serum. In addition, they could also increase the expression of G-CSF and GM-CSF in the bone marrow, thereby play a role in

promoting the recovery of bone marrow hematopoietic function. Ferulic acid could increase the levels of G-CSF and EPO, enhance the activity of HSCs, and accelerate the recovery of peripheral blood cells. Calycosin glucoside increased the levels of RBC and HGB in myelosuppressed mice, promoted the secretion of EPO and EPO, and promoted the proliferation of hematopoietic cells, thereby promoting the recovery of hematopoietic function.

To test the hypotheses of network pharmacology and molecular docking, in vitro experiments were conducted. BMSCs play an important role in promoting the homing, regeneration, and functional recovery of HSCs, which are closely related to the hematopoietic function of the bone marrow.[40] Studies have shown that the PI3K-Akt signaling pathway could be involved in regulating the survival, differentiation, proliferation, and migration of BMSCs. And SYD could promote cell proliferation, inhibit cell apoptosis, increase the secretion of hematopoietic growth factors and improve the bone marrow hematopoietic microenvironment.[41] Therefore, combined with our results of network pharmacology, we speculate that SYD may play a role in the treatment of myelosuppression by activating PI3K-Akt pathway, regulating the process of cell proliferation and apoptosis. OP9 cells can support embryonic-derived stem cells to develop into hematopoietic cells, and co-culture with OP9 induces the differentiation of hematopoietic stem/progenitor cells,[42] which are widely used in related studies on hematopoietic development and differentiation. Therefore, OP9 cells were selected for in vitro validation in this study. While killing tumor cells, 5-FU also causes oxidative damage to BMSCs, changes the secretion of bioactive substances, and induces premature aging of hematopoietic cells.[43] Thus, 5-FU was used as a modeling agent to establish myelosuppressive OP9 cells. In this study, we verified the effectiveness of the predicted components using OP9 cells. The results showed that ferulic acid, paeoniflorin, albiflorin, and calycosin-7-O-glucoside could all promote the proliferation of myelosuppressive OP9 cells, and among them albiflorin had the strongest effect, which was selected to act the follow-up mechanism study. Our research found that Albiflorin promoted OP9 cell proliferation and reduced apoptosis. When the PI3K-Akt pathway was inhibited, the protective effects of albiflorin on OP9 cells were also inhibited, and the protein expression levels of PI3K, p-PI3K, Akt, and p-Akt were significantly decreased, whereas when the pathway was activated, the protein expression and phosphorylation levels were increased. Therefore, it is speculated that albiflorin could activate the PI3K-Akt signaling pathway and increase the phosphorylation level of Akt, thereby play a role in promoting proliferation and anti-apoptosis by regulating the expression of corresponding proteins in BMSCs. This indicates that activation of the PI3K-Akt pathway may be one of the mechanisms by which albiflorin treats CIM. The in vitro validation results were consistent with our hypothesis.

Conclusion

In Conclusion, this study revealed the active components of SYD and its potential therapeutic targets in myelosuppression by integrating network, molecular docking, and experimental pharmacology. The LC-QTOF/MS results provided a material basis for subsequent research on SYD. Network pharmacology and molecular docking results indicated that the regulation of cell proliferation and apoptosis by the PI3K-Akt signaling pathway is a key biological process by which SYD protects against myelosuppression. Moreover, calycosin-7-glucoside, ferulic acid, albiflorin, and paeoniflorin were predicted to be the active constituents of SYD against myelosuppression. Finally, the proliferation and anti-apoptotic effects of the active components of SYD were tested in vitro, which validated the protective effect of SYD against myelosuppression. In summary, our study provides evidence supporting the therapeutic effect of SYD and provides a pharmacological and material basis for its use in the treatment of myelosuppression, which would contribute to the modern research and clinical application of SYD.

Acknowledgments

This work was supported by the National Natural Science Foundation of China (Nos. 81673510 and 82073936), the Outstanding Scientific Fund of Shengjing Hospital (No. M0779), and Characteristic Innovation Project of the Guangdong Provincial Education Department (No. 2019GKTSCX039 and 200KTSCX295).

Disclosure

The authors declare that there are no conflicts of interest in this work.

References

1. Han J, Xia J, Zhang L, et al. Studies of the effects and mechanisms of ginsenoside Re and Rk3 on myelosuppression induced by cyclophosphamide. *J Ginseng Res*. 2019;43(4):618–624. doi:10.1016/j.jgr.2018.07.009
2. Chen X, Li B, Gao Y, Ji J, Wu Z, Chen S. Saponins from Sanguisorba officinalis Improve Hematopoiesis by promoting survival through FAK and Erk1/2 activation and modulating cytokine production in bone marrow. *Front Pharmacol*. 2017;8:130. doi:10.3389/fphar.2017.00130
3. Park MH, Jung IK, Min WK, et al. Neuropeptide Y improves cisplatin-induced bone marrow dysfunction without blocking chemotherapeutic efficacy in a cancer mouse model. *BMB Rep*. 2017;50(8):417–422. doi:10.5483/bmbrep.2017.50.8.099
4. Anisimova N, Ustyuzhanina N, Bilan M, et al. Fucoidan and fucosylated chondroitin sulfate stimulate hematopoiesis in cyclophosphamide-induced mice. *Mar Drugs*. 2017;15(10):301. doi:10.3390/md15100301
5. He M, Wang N, Zheng W, et al. Ameliorative effects of ginsenosides on myelosuppression induced by chemotherapy or radiotherapy. *J Ethnopharmacol*. 2021;268:113581. doi:10.1016/j.jep.2020.113581
6. Wang S, Xu Z, Wang L. Shuanghuang Shengbai granule cures myelosuppression and suppresses lung cancer progression: mechanism and therapeutic targets from the aspect of microRNAs. *Oncotarget*. 2017;8(37):62154–62166. doi:10.18632/oncotarget.19129
7. Zhang S, Mi Y, Ye T, et al. Carbohydrates and ginsenosides in shenmai injection jointly improve hematopoietic function during chemotherapy-induced myelosuppression in mice. *Chin Med*. 2022;17(1):124. doi:10.1186/s13020-022-00678-5
8. Liu Y, Chang M, Hu Z, et al. Danggui Buxue Decoction enhances the anticancer activity of gemcitabine and alleviates gemcitabine-induced myelosuppression. *J Ethnopharmacol*. 2021;273:113965. doi:10.1016/j.jep.2021.113965
9. Zhang Y, Ye T, Hong Z, et al. Pharmacological and transcriptome profiling analyses of Fufang E'jiao Jiang during chemotherapy-induced myelosuppression in mice. *J Ethnopharmacol*. 2019;238:111869. doi:10.1016/j.jep.2019.111869
10. Chen L, Song M, Zhang LS, et al. The protective effects of different compatibility proportions of the couplet medicines for astragali radix and angelica sinensis radix on myocardial infarction injury. *Pharm Biol*. 2020;58(1):165–175. doi:10.1080/13880209.2020.1725581
11. Zheng HZ, Fu XK, Shang JL, et al. Ginsenoside Rg1 protects rat bone marrow mesenchymal stem cells against ischemia induced apoptosis through miR-494-3p and ROCK-1. *Eur J Pharmacol*. 2018;822:154–167. doi:10.1016/j.ejphar.2018.01.001
12. Zheng YJ, Ren WY, Zhang LN, et al. A review of the pharmacological action of astragalus polysaccharide. *Front Pharmacol*. 2020;11(349):2–15. doi:10.3389/fphar.2020.00349
13. Gu X, Zhu LY, Xu ZY, et al. Astragaloside IV and saponins of rhizoma polygonati cure cyclophosphamide-induced myelosuppression in lung adenocarcinoma via down-regulating miR-142-3p. *Front Oncol*. 2021;11:630921. doi:10.3389/fonc.2021.630921
14. He S, Wang T, Shi C, Wang Z, Fu X. Network pharmacology-based approach to understand the effect and mechanism of Danshen against anemia. *J Ethnopharmacol*. 2022;282:114615. doi:10.1016/j.jep.2021.114615
15. Aihaiti Y, Song Cai Y, Tuerhong X, et al. Therapeutic Effects of naringin in rheumatoid arthritis: network pharmacology and experimental validation. *Front Pharmacol*. 2021;12:672054. doi:10.3389/fphar.2021.672054
16. Vaijanathappa J, Puttaswamygowda J, Bevanhalli R, Dixit S, Prabhakaran P. Molecular docking, antiproliferative and anticonvulsant activities of swertiamarin isolated from Enicostemma axillare. *Bioorg Chem*. 2020;94:103428. doi:10.1016/j.bioorg.2019.103428
17. Zhou W, Dai Y, Meng J, et al. Network pharmacology integrated with molecular docking reveals the common experiment-validated antipyretic mechanism of bitter-cold herbs. *J Ethnopharmacol*. 2021;274:114042. doi:10.1016/j.jep.2021.114042
18. Liu H, Hu Y, Qi B, et al. Network pharmacology and molecular docking to elucidate the mechanism of pulsatilla decoction in the treatment of colon cancer. *Front Pharmacol*. 2022;13:940508. doi:10.3389/fphar.2022.940508
19. Lin Y, Shen C, Wang F, Fang Z, Shen G. Network pharmacology and molecular docking study on the potential mechanism of Yi-Qi-Huo-Xue-Tong -Luo formula in treating diabetic peripheral neuropathy. *J Diabetes Res*. 2021;2021:9941791. doi:10.1155/2021/9941791
20. Li Y, Wang Y, Tai W, et al. Challenges and solutions of pharmacokinetics for efficacy and safety of traditional Chinese medicine. *Curr Drug Metab*. 2015;16(9):765–776. doi:10.2174/1389200216091512011142 23
21. Polettini AE, Kutzler J, Sauer C, Bleicher S, Schultis W. LC-QTOF-MS presumptive identification of synthetic cannabinoids without reference chromatographic retention/mass spectral information. I. Reversed-phase retention time QSPR prediction as an aid to identification of new/unknown compounds. *J Anal Toxicol*. 2021;45(5):429–439. doi:10.1093/jat/bkaa126
22. Vikingsson S, Rautio T, Wallgren J, et al. LC-QTOF-MS identification of major urinary cyclopropylfentanyl metabolites using synthesized standards. *J Anal Toxicol*. 2019;43(8):607–614. doi:10.1093/jat/bkz057
23. Ferrarotto R, Anderson I, Medgyasszay B, et al. Trilaciclib prior to chemotherapy reduces the usage of supportive care interventions for chemotherapy-induced myelosuppression in patients with small cell lung cancer: pooled analysis of three randomized Phase 2 trials. *Cancer Med*. 2021;10(17):5748–5756. doi:10.1002/cam4.4089
24. Kang M, Park S, Chung Y, Lim J-O, Kang JS, Park JH. Hematopoietic effects of angelica gigas Nakai extract on cyclophosphamide-induced myelosuppression. *Plants*. 2022;11(24):3476. doi:10.3390/plants11243476
25. Chuang CH, Lin YC, Yang J, Chan ST, Yeh SL. Quercetin supplementation attenuates cisplatin induced myelosuppression in mice through regulation of hematopoietic growth factors and hematopoietic inhibitory factors. *J Nutr Biochem*. 2022;110:109149. doi:10.1016/j.jnutbio.2022.109149
26. Huang Q, Feng L, Li H, et al. Jian-Pi-Bu-Xue-formula alleviates cyclophosphamide-induced myelosuppression via up-regulating NRF2/HO1/NQO1 Signaling. *Front Pharmacol*. 2020;11:1302. doi:10.3389/fphar.2020.01302
27. Gong PY, Tian YS, Guo YJ, et al. Comparisons of antithrombosis, hematopoietic effects and chemical profiles of dried and rice wine-processed rehmanniae radix extracts. *J Ethnopharmacol*. 2019;231:394–402. doi:10.1016/j.jep.2018.10.025
28. Liu C, Li J, Meng FY, et al. Polysaccharides from the root of Angelica sinensis promotes hematopoiesis and thrombopoiesis through the PI3K/AKT pathway. *BMC Complement Altern Med*. 2010;10:79. doi:10.1186/1472-6882-10-79
29. Sun X, Zhao YN, Qian S, et al. Ginseng-derived panaxadiol saponins promote hematopoiesis recovery in cyclophosphamide-induced myelosuppressive mice: potential novel treatment of chemotherapy-induced cytopenias. *Chin J Integr Med*. 2018;24(3):200–206. doi:10.1007/s11655-017-2754-8
30. Guo K, Wang T, Luo E, et al. Use of network pharmacology and molecular docking technology to analyze the mechanism of action of velvet antler in the treatment of postmenopausal osteoporosis. *Evid Based Complement Alternat Med*. 2021;11:7144529. doi:10.1155/2021/7144529

31. Jiang YH, Jhang JF, Hsu YH, Kuo HC. Usefulness of urinary biomarkers for assessing bladder condition and histopathology in patients with interstitial cystitis/bladder pain syndrome. *Int J Mol Sci*. 2022;23(19):12044. doi:10.3390/ijms231912044
32. Li L, Rispoli R, Patient R, et al. Etv6 activates vegfa expression through positive and negative transcriptional regulatory networks in Xenopus embryos. *Nat Commun*. 2019;10(1):1083. doi:10.1038/s41467-019-09050-y
33. Zeng X, Yu SP, Taylor T, et al. Protective effect of apelin on cultured rat bone marrow mesenchymal stem cells against apoptosis. *Stem Cell Res*. 2012;8(3):357–367. doi:10.1016/j.scr.2011.12.004
34. Perry JM, He XC. Cooperation between both Wnt/{beta}-catenin and PTEN/PI3K/Akt signaling promotes primitive hematopoietic stem cell self-renewal and expansion. *Genes&development*. 2011;25(18):1928–1942. doi:10.1101/gad.17421911
35. Shen GY, Ren H, Huang JJ, et al. Plastrum testudinis extracts promote BMSC proliferation and osteogenic differentiation by regulating Let-7f-5p and the TNFR2/PI3K/Akt signaling pathway. *Cell Physiol Biochem*. 2018;47(6):2307–2318. doi:10.1159/000491541
36. Zhu Y, Wang L, Yang Z, et al. Hematopoietic effects of paeoniflorin and albiflorin on radiotherapy-induced myelosuppression mice. *Evid Based Complement Alternat Med*. 2016;5789381. doi:10.1155/2016/5789381
37. Das U, Manna K, Khan A, et al. Ferulic acid (FA) abrogates γ-radiation induced oxidative stress and DNA damage by up-regulating nuclear translocation of Nrf2 and activation of NHEJ pathway. *Free Radic Res*. 2017;51(1):47–63. doi:10.1080/10715762.2016.1267345
38. Ma ZC, Hong Q, Wang YG, et al. Effects of ferulic acid on hematopoietic cell recovery in whole-body gamma irradiated mice. *Int J Radiat Biol*. 2011;87(5):499–505. doi:10.3109/09553002.2011.548438
39. Zhang W, Zhu JH, Xu H, et al. Five active components compatibility of astragali radix and angelicae sinensis radix protect hematopoietic function against cyclophosphamide-induced injury in mice and t-BHP-Induced Injury in HSCs. *Front Pharmacol*. 2019;22(10):936. doi:10.3389/fphar.2022.1051973
40. Xiao Y, Wang Y, Li L, et al. Homing of chloromethylbenzoyl ammonia-labeled bone marrow mesenchymal stem cells in an immune-mediated bone marrow failure mouse model in vivo. *Genet Mol Res*. 2014;13(1):11–21. doi:10.4238/2014
41. Zhao J. *Effect of Shengyu Traditional Decoction and Shengyu Formula Granula on Hematopoietic Regulation in Myelosuppressed Mice*. Chengdu University of Traditional Chinese Medicine; 2011.
42. Hirota S, Ogawa M. Activin A in combination with OP9 cells facilitates development of Flk-1(+) PDGFRα(-) and Flk-1(+) PDGFRα(+) hematopoietic mesodermal cells from murine embryonic stem cells. *Biochem Biophys Res Commun*. 2015;467(3):583–588. doi:10.1016/j.bbrc.2015.09.131
43. Xiao H, Xiong LR, Song XY, et al. Angelica sinensis polysaccharides ameliorate stress-induced premature senescence of hematopoietic cell via protecting bone marrow stromal cells from oxidative injuries caused by 5-fluorouracil. *Int J Mol Sci*. 2017;18(11):2265. doi:10.3390/ijms18112265